# Electronic Structures and Linear Optics of $A_2B_2O_5$ (A = Mg, Ca, Sr) Pyroborates

W.-D. Cheng,* H. Zhang, F.-K. Zheng, J.-T. Chen, Q.-E. Zhang, and R. Pandey†

*Fujian Institute of Research on the Structure of Matter, Chinese Academy of Sciences, State Key Laboratory of Structural Chemistry, Fuzhou, Fujian 350002, People's Republic of China*

*Received February 29, 2000. Revised Manuscript Received August 21, 2000*

The electronic structure and linear optical properties of the pyroborate $A_2B_2O_5$ (A = Mg, Ca, Sr) compounds are reported here. These compounds, which crystallize with four formula units in the monoclinic space group $P2_1/c$, are modeled in terms of the cluster units $(A_2B_2O_5)_2$. The calculated electronic structures show that the top of the valence band consists of mostly the O-2p orbitals and the bottom of the conduction band consists of cationic orbitals. The dynamic refractive indices of these pyroborates are obtained in the framework of the INDO/SCI approximation together with the sum-over-states method. It is found that the refractive index increases with an increase of alkaline-earth cationic radius for pyroborates, and the charge-transfer for $O^{2-}$ anion orbitals to $A^{2+}$ cation orbitals appears to provide a significant contribution to the linear polarizability of these compounds.

## 1. Introduction

Solid-state borates have become a focus of technological interest due to a variety of physical and chemical features exhibited by these componds, such as the luminescence of tetraborate $SrB_4O_7$,[1,2] the nonlinear optical properties[3] of the $(B_3O_6)^{3-}$ group in borates, and the catalytic activity of the copper borate $Cu_2Al_6B_4O_{17}$.[4] Among the nonlinear optical crystals, solid-state borates have emerged as the preeminent materials for high-power applications, and now they are being utilized in the manufacture of components in essentially all complex microprocessor-based devices from PCs to cellular phones. Keszler and co-workers have systematically investigated the syntheses, structures, and properties of alkali-metal pyroborates, searching for a trend in the structure−property relationship.[5,6] Cheng et al. have calculated the electronic structure and nonlinear optical coefficients of $CsB_3O_5$, $LiB_3O_5$, and $CsLiB_3O_5$ with an aim to understand the electronic origin of their optical susceptibility.[7] Thompson et al.[8] have discussed the unusual features and significance of the pyroborate geometry, suggesting that a more highly coplanar arrangement of $B_2O_5$ group should produce a larger birefringence in these compounds. It is well-known that the increasing size of the alkali-metal cation has introduced a relatively more coplanar arrangement of the group $B_2O_5$ in pyroborates.[5] The simplest condensation of a triangular group in borate chemistry facilitates the pyroborate anion $B_2O_5^{4-}$. In the pyroborates lattice,[8] the terminal $BO_2$ planes pivot about the torsion angles to afford deviations from coplanarity that range from 1.6° to 67.0°, while the central B−O−B angle ranges from 111.8° to 138.7°. The pyroborate groups do not pack in distinct layers and are coupled with a suitable constructive summation of microscopic hyperpolarizability coefficients after interacting with cations. This coupling results in a useful material with characteristics of a small threshold for conversion and relatively less angular sensitivity to phase matching.

In this paper we use a cluster unit representing the crystalline pyroborate lattice to calculate the electronic structure and refractive indices of alkali-earth metal pyroborates $A_2B_2O_5$ (A = Mg, Ca, Sr). These compounds have been synthesized by high-temperature solution reactions and structurally characterized by single-crystal X-ray diffraction in our group.[9] The calculated results show the ion-size effect of cations on both band gap and refractive index, indicating an increase of the refractive index with an increase of alkaline-earth cation radius in pyroborates.

## 2. Computational Procedures

The electronic structural calculations of the cluster units (i.e. microspecies of the title compounds) were based on an all-valence-electron, semiempirical INDO

* To whom correspondence should be addressed.
† Present address: Department of Physics, Michigan Technological University, Houghton, MI 49931.

(1) Blasse, G.; Dirksen, G. J.; Meijerink, A. *Chem. Phys. Lett.* **1990**, *167*, 41−44.
(2) Meijerink, A.; Nuyten, J.; Blasse, G. *J. Lumin.* **1989**, *44*, 19−31.
(3) Chen, C.-Z.; Gao, D.-S.; Chen, C.-T. *Academic Thesis Conf. Cryst. Growth Mater. (China)* **1979**, *B44*, 107−111.
(4) Zletz, A. (Amoco Corp.), *U.S. Patent Application* 709, 790, 11 March 1985.
(5) Akella, A.; Keszler, D. A. *J. Solid State Chem.* **1995**, *120*, 74−79.
(6) Smith, R. W.; Keszler, D. A. *J. Solid State Chem.* **1997**, *129*, 184−188.
(7) Cheng, W.-D.; Chen, J.-T.; Lin, Q.-S.; Zhang, Q.-E.; Lu, J.-X. *Phy. Rev. B* **1999**, *60*, 11747−11754.
(8) Thompson, P. D.; Huang, J.; Smith, R. W.; Keszler, D. A. *J. Solid State Chem.* **1991**, *95*, 126−135.
(9) (a) Guo, G.-C.; Cheng, W.-D.; Chen, J.-T.; Zhuang, H.-H.; Huang, J.-S.; Zhang, Q.-E. *Acta Crystallogr.* **1995**, *C* 51, 2469−2471. (b) Lin, Q.-S.; Cheng, W.-D.; Chen, J.-T.; Huang, J.-S. *Acta Crystallogr.* **1999**, *C* 55, 4-6. (c) Lin, Q.-S.; Cheng, W.-D.; Chen, J.-T.; Huang, J.-S. *J. Solid State Chem.* **1999**, *144*, 30−34.

10.1021/cm000188l CCC: $19.00 
Published on Web 11/16/2000

**Table 1. INDO/S Model Parameters**

| parameter | B | O | Mg | Ca | Sr |
|---|---|---|---|---|---|
| $\zeta_{ns,np}$ (Å$^{-1}$) | 1.300 | 2.275 | 1.103 | 1.210 | 1.214 |
| $\zeta_{(n-1)d}$ (Å$^{-1}$) | | | | 1.850 | 2.058 |
| $-I_{ns}$ (ev) | 14.05 | 32.90 | 8.11 | 6.03 | 5.84 |
| $-I_{np}$ (ev) | 8.70 | 17.28 | 4.55 | 3.96 | 3.76 |
| $-I_{(n-1)d}$ (ev) | | | | 3.44 | 3.66 |
| $-\beta_{ns,np}$ (ev) | 17.00 | 34.20 | 6.0 | 2.0 | 1.88 |
| $-\beta_{(n-1)d}$ (ev) | | | | 12.05 | 10.05 |
| $\gamma_{ns,np}$ (ev) | 8.68 | 13.00 | 4.79 | 3.25 | 3.75 |
| $\gamma_{(n-1)dd}$ (ev) | | | | 6.03 | 5.31 |
| $\gamma_{(n-1)dns,np}$ (eV) | | | | 4.00 | 4.53 |

self-consistent field (SCF) molecular orbital (MO) procedure with the configuration interaction (CI) method as modified by Zerner and co-workers.[10−13] There are the one-center core integral, $U_{\mu\mu}$; resonance integral, $\beta_{\mu\nu}$; two-electron integral, $\gamma_{\mu\nu}$; overlap integral, $S_{\mu\nu}$; and density matrix element, $P_{\mu\nu}$, in the matrix element of the Fock operator under the INDO approximation. The INDO model as employed herein included all one-center, two-electron integrals and all two-center, two-electron integrals, $\gamma_{\mu\nu}$. The one-center, two-electron integrals, $\gamma_{\mu\mu}$, were chosen from the Pariser approximation, $\gamma_{\mu\mu} = F_0(\mu\mu) = IP_\mu - EA_\mu$, and the two-center, two electron integrals were calculated using the Mataga−Nishimoto formula, $\gamma_{\mu\nu} = 1.2/[R_{AB} + 2.4/(\gamma_{\mu\mu} + \gamma_{\nu\nu})]$, in the spectroscopic version of INDO method. The Slater orbital exponents, $\zeta$, and the other calculating parameters are listed in Table 1. The molecular orbital calculations were performed by the restricted Hartree−Fock method. The ground state was constructed as single-determinant, obtained from the Hartree−Fock SCF calculated results. Only single-substituted determinants relative to the ground state configuration were considered, and only singlet spin-adapted configurations needed to be included in the CI calculations. The ground state and all excited states had the multiplicity of 1. The electron was promoted from the 13 highest occupied orbitals to the 13 lowest unoccupied orbitals, and the configuration space was constructed by these 26 active orbitals. The wave functions and energy eigenvalues of the excited states were determined by solving the secular equation relating to configuration coefficients. The dipole and transition moment matrix elements were expressed as a sum of one-electron integrals.

The tensor components of the polarizability, $\alpha(\omega)$, with frequency dependence for the microspecies of the title compounds were calculated by the sum-over-states (SOS) method as follows:

$$\alpha_{ij}(\omega) = 1/\hbar \Sigma_m \mu_{gm}^{\,i} \mu_{mg}^{\,j} [(\omega_{mg} - \omega_p)^{-1} + (\omega_{mg} + \omega_p)^{-1}] \quad (1)$$

The cluster units $(A_2B_2O_5)_2$, representing extended oxide crystals $A_2B_2O_5$ (A = Mg, Ca, Sr) were chosen for calculations. Theoretical calculations of electronic structure and polarizabilities are based on the crystallographic structural data for these clusters, whose coordinates can be obtained from our group.[9]

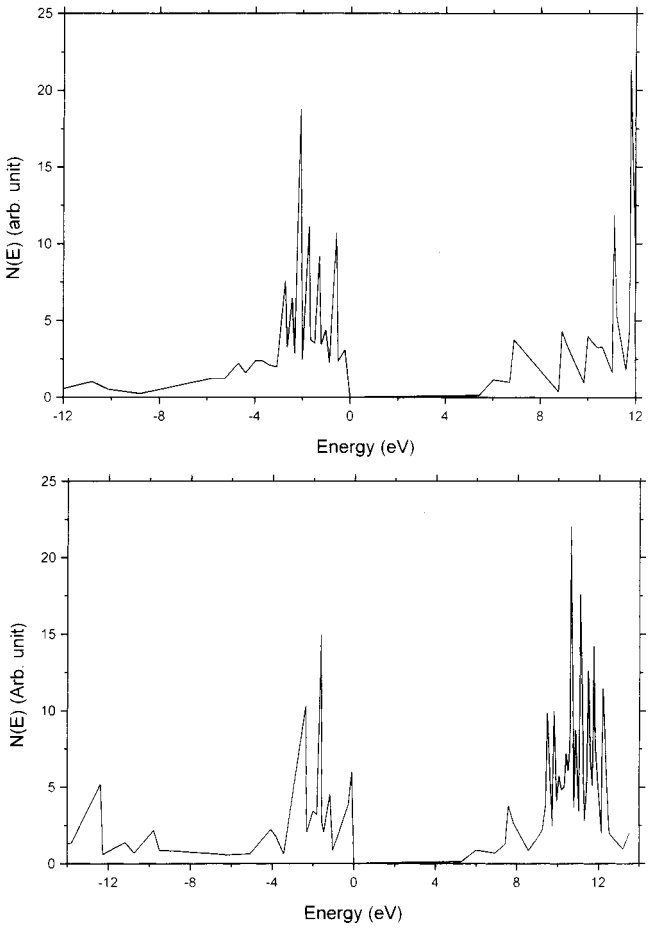


**Figure 1.** (a) Atomic state density of $Mg_2B_2O_5$. (b) State density of $Ca_2B_2O_5$.

## 3. Results and Discussions

**3.1. Electronic Structures.** The energy bands for $Mg_2B_2O_5$, and $Ca_2B_2O_5$ are calculated here, while that for $Sr_2B_2O_5$ is taken from our previos work given in ref 9c. Note that the top of the valence band of $Mg_2B_2O_5$, and $Ca_2B_2O_5$ is at −6.78 and −5.55 eV, respectively; these are taken to be zero and regarded as a reference in the following discussion.

In $Mg_2B_2O_5$, the dominant contribution to the lower valence band (i.e. −29.8 to −23.0 eV) comes from O-2*s* orbitals along with a relatively small (6%) contrbution from B-2*s* orbitals. It is therefore assigned as an s valence band. The upper valence band ranging from −12.2 to 0.00 eV is a result of contributions from O-2*p* orbitals that are mixed with B-2*p* orbitals (less than 12%). The atomic state density of the upper valence band is displayed in Figure 1a. Here, the $\sigma$-bonding interactions between the O-2*p* and B-2*p* orbitals yield the peaks ranging from −12.2 to −5.2 eV. On the other hand, the peaks localized in the energies from −4.7 to −1.7 eV can be assigned to the $\pi$-bonding interactions between the O-2*p* and B-2*p* orbitals. Finally, the 2*p* orbitals of the terminal oxygen atoms dominate the region from −1.5 eV to the top of the valence band. Figure 1a also includes the atomic state density of the lower conduction band (CB). Here, the peaks localized

(10) Bacon, A. D.; Zerner, M. C. *Theor. Chim. Acta* **1979**, *53*, 21−54.
(11) Zerner, M. C.; Lovw, G. H.; Kirchner, R. F.; Mueller-Westerhoff, U. T. *J. Am. Chem. Soc.* **1980**, *102*, 589−599.
(12) Anderson, W. P.; Edwards, E. D.; Zerner, M. C. *Inorg. Chem.* **1986**, *25*, 2728−2732.
(13) Anderson, W. P.; Cundari, T. R.; Zerner, M. C. *Int. J. Quantum Chem.* **1991**, *39*, 31−45.

in the energy region between 5.4 and 12.9 eV are mainly due to contributions from the magnesium ionic state. For example, the peak localized at 6.9 eV has contributions of about 54% from Mg-3s orbital and the peak localized at 11.8 eV has contribution of about 57% from Mg-3p orbitals. The conduction band region ranging from 13.3 to 18.7 eV is formed by the antibonding interactions between the orbitals of boron (>42% of 2s and 2p characters) and oxygen (<21% of 2p character). The calculated gap between the top of the valence band and the bottom of the conduction band comes out to be 5.44 eV, yielding the absorption edge of $Mg_2B_2O_5$ crystal at about 228 nm.

In $Ca_2B_2O_5$, the valence band ranging from −30.1 to 0.0 eV (Figure 1b) can also be divided into s- and p-subbands. The main contributions in the s-band are from (71−86%) O-2*s* and B-2*s* valence orbitals. On the other hand, contributions from three types of orbital interactions are seen in the p-subband. The $\sigma$-bonding interactions between the O-2p and B-2p orbitals contribute in the lowest energy region of the p-subband. For example, the peak localized at about −12.4 eV has a character of about 53% O-2*p* and 25% B-2*p* orbitals. The band from −8.8 to −3.4 eV is mainly due to the $\pi$-bonding interactions between the O-2*p* and B-2*p* orbitals. The band between the energies −2.4 and 0.0 eV is assigned to the 2*p* orbitals of the terminal oxygen atoms. The lower conduction band which ranges from 5.3 and 14.6 eV has contributions from the calcium ionic state. The band from 5.3 to 7.4 eV is mainly due to Ca-4*s* orbitals, whereas Ca-3d and Ca-4*p* orbitals contribute to the band up to 14.2 eV. The next band (19.7−26.7 eV) is formed by the antibonding interactions between the boron (>58% of 2*s* and 2*p* characters) and oxygen (<42% of 2p character) orbitals. The minimum energy gap between the top of the valence band and the bottom of the conduction band is calculated to be 5.30 eV, yielding the absorption edge of $Ca_2B_2O_5$ to be about 234 nm.

The calculated band structure[9c] of $Sr_2B_2O_5$ is found to be similar to those obtained for $Mg_2B_2O_5$ and $Ca_2B_2O_5$ ($A$ = Mg, Ca). Here, a larger (smaller) contribution to the bands comes from the more electronegative O atom in the valence band (conduction band). The calculated minimum energy gap is found to be 4.26 eV.

**3.2. Optical Properties.** The optical properties of a bulk material can be thought of as being built up from the corresponding properties of individual cluster units or microscopic species. In this approximation, the linear refractive index can be written as

$$n^2(\omega) = 1 + 4\pi\chi^{(1)}(\omega) \qquad (2)$$

where the linear susceptibility $\chi^{(1)}(\omega)$ is defined as

$$\chi^{(1)}(\omega) = N\alpha(\omega)/[1 - (4\pi/3)N\alpha(\omega)] \qquad (3)$$

Here, $\alpha(\omega)$ is the frequency-dependent polarizability and $N$ is the cluster number density. For the usual case in which the polarizability $\alpha(\omega)$ is positive, we see that the susceptibility is larger than the value $N\alpha(\omega)$ predicted by calculations that ignore local-field corrections. The cluster number density, $N$, can be obtained by a product of mass density and Avogadro's number, that, is dividing by molar mass. For $(Mg_2B_2O_5)_2$, with a molecular formula weight of 300.48 g/mol and a mass density of 2.91 g/cm$^3$, we obtain $N = 5.832 \times 10^{21}$ cm$^{-3}$. The $N$ is calculated to be $4.671 \times 10^{21}$ cm$^{-3}$ and $4.089 \times 10^{21}$ cm$^{-3}$ for the $(Ca_2B_2O_5)_2$ and $(Sr_2B_2O_5)_2$, respectively. It is to be noted here that, through rearrangement of the Lorentz−Lorenz equation, $(\epsilon^{(1)} - 1)/(\epsilon^{(1)} + 2) = 4/3\pi N\alpha$, we can obtain the relationship $(\epsilon^{(1)} + 2)/3 = 1/[1 - (4\pi/3)N\alpha]$.[14] Accordingly, the factor $1/[1 - (4\pi/3)N\alpha]$ or $(\epsilon^{(1)} + 2)/3$ is interpreted as the local-field correction factor for the linear susceptibility and can be described as the interaction between a selected cluster unit and the surrounding environment. In fact, the determination of the local field factor can be quite complicated for a condensed system.[15,16] We only take an approximate treatment of a spherical cavity to obtain the local field factor[17] in this study.

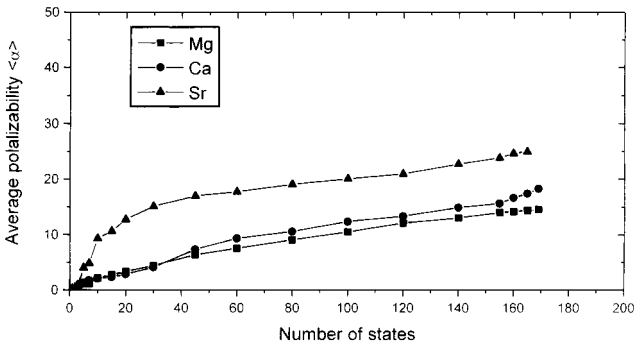


**Figure 2.** The polarizability $\langle\alpha\rangle$ of clusters at $\lambda = 1064$ nm.

Before attempting to compute the frequency dependence of the refractive index for pyroborates, it is necessary to investigate the convergence behavior in the summation of excited states of clusters $(A_2B_2O_5)_2$ ($A$ = Mg,Ca,Sr). This exercise will help us in determining the reliabilty of the INDO/SCI method used here. Figure 2 shows the calculated average polarizability $\langle\alpha\rangle$ versus the number of states for $(A_2B_2O_5)_2$ ($A$ = Mg,Ca,Sr) at 1064 nm. Accordingly, $\langle\alpha\rangle$ is converging very slowly, though it has reached the stability after summation over 150 states. It is well-known that the sum-over-states expansion in eq 1 is, in general, infinite, since the applied optical field mixes the ground state to several excited states. Combining the results of Figure 2 with the state density of Figure 1, we can identify that the charge transfer from the O-2p orbitals to alkaline-earth valence orbitals is the dominant contributor to the calculated linear polarizabilities.

The average dynamic refractive index of $\langle n(\alpha)\rangle$ was calculated using a general definition for the average polarizability (i.e. $\langle\alpha\rangle = (\alpha_{xx}+\alpha_{yy}+\alpha_{zz})/3$) and eqs 2 and 3. Figure 3 shows the refractive indices $\langle n(\alpha)\rangle$ of $Mg_2B_2O_5$, $Ca_2B_2O_5$, and $Sr_2B_2O_5$ for wavelengths ranging from 0.40 to 5.0 mm. It is found that the refractive index increases with an increase of alkaline-earth ionic radius for pyroborates. The observed refractive index of $Mg_2B_2O_5$, $n_x$, $n_y$, $n_z$, is individually 1.589, 1.660, 1.674,

(14) Boyd, Robert W. *Nolinear Optics*; Academic Press: San Diego, CA, 1992; p 148.
(15) Munn, R. *Int. J. Quantum Chem*. **1992**, *43*, 159−169.
(16) Sylvester-Hvid, K. D.; Mikkelsen, K. V.; Patrick, D. J.; Agren, H. J. *J. Phys. Chem. A* **1999**, *103*, 8375−8383.
(17) Burland, D. M.; Miller, R. D.; Walsh C. A. *Chem. Rev.* **1994**, *94*, 31−75.

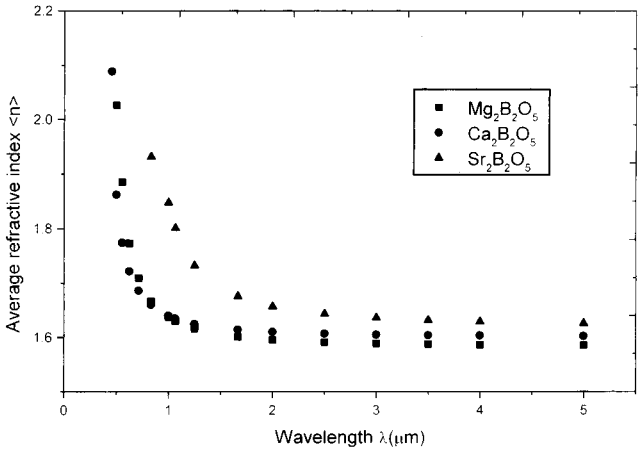


**Figure 3.** The calculated dynamic refractive index.

and the average refractive index is 1.641,[18] the calculated refractive index, $n_x$, $n_y$, $n_z$ is individually 1.413, 1.692, 1.818, and the average $\langle n \rangle$ is 1.641 at 1.065 $\mu$m. Given the approximations involved in the computational model used here, the agreement between calculation and experiment seems to be satisfactory.

(18) Davis, H. M.; Knight, M. A. *J. Am. Ceram. Soc.* **1945**, *28*, 97–102.

## 4. Conclusions

In this work, the cluster units $(A_2B_2O_5)_2$ are chosen to calculate the electronic structure and refractive indices of the $A_2B_2O_5$ (A = Mg,Ca,Sr) pyroborates. Electronic structure calculations find that the lower valence band is derived from O-2s and B-2s orbitals, whereas the upper valence band is formed by the bonding interactions between the O-2p and B-2p orbitals. The charge transfer from O-2p orbitals to cationic orbitals is found to make significant contributions to the calculated refractive index of these compounds. As the size of the alkaline-earth cation increases in the pyroborate series considered here, the calculated minimum energy gap decreases and the calculated average refractive index increases.

**Acknowledgment.** This investigation was supported by the National Science Foundation of China (No. 29973048) and the Foundation of State Key Laboratory of Structural Chemistry (No. 200027).

CM000188L